Study of Surface Roughness Effects in Elastohydrodynamic Lubrication of a Finite Line Contact Using Probabilistic Model

S.P. Chippa
Department of Mechanical Engineering
Vishwakarma Institute of Technology, Pune
Maharashtra, India
chippashriniwas@gmail.com

M. Sarangi
Department of Mechanical Engineering
Indian Institute of Technology, Kharagpur
West Bengal, India
smihir@mech.iitkgp.ernet.in

***Abstract*—A numerical solution is obtained for fully flooded isothermal elastohydrodynamically lubricated finite line contact including surface roughness effect (Patir-Cheng flow model). It is observed that the maximum pressure and minimum film thickness appears along the edges of the cylindrical roller, which cannot be predicted by infinite line contact analysis (1D). A significant difference in the film thickness results of finite and infinite contact are reported, particularly for lower values of hydrodynamic roughness parameter Λ. Based on the numerically evaluated data, curve fitted relations for central and central minimum film thicknesses are developed by using a non-linear least square technique.**

Keywords—EHL; Finite line contact; Surface roughness

I. INTRODUCTION

Machine elements like roller bearings, cam-followers, traction drives, gears are traditionally analysed using elastohydrodynamically lubricated (EHL) infinite line contact theory, which assumes the contacting elements to be infinitely long in one of the principal direction i.e. along the length of the roller. In reality, infinitely long line contact can hardly be in existence. In fact, the contact length is always finite and moreover, the rollers are axially profiled at the two ends for reduction of stress concentration. Dub-off and partially crowned profiles are the commonly used edge profiles by the bearing manufactures due to easiness in their processability [1]. However, these edge profiles are an approximation to the theoretical Lundberg's profile [2]. In the past research publications, few studies have been reported on the EHL finite line contact for smooth surfaces [3-6].

Nowadays, the industrial applications of lubrication demands for the EHL contacts to perform under more severe load condition without compromising the efficiency. Under such heavy loads, the fluid film thickness between the rolling contacts is comparable with the combined roughness of contacting surfaces. Therefore, it becomes essential to include the surface roughness effect in the EHL analysis in order to set the design parameters. There are two approaches for analysing rough surface EHL contacts, namely probabilistic approach and deterministic approach. In the deterministic approach, large mesh size is essential for an accurate representation of the roughness profiles which takes large computational time.

The study of rough surface EHL contacts was initiated with probabilistic approach. In this method the derivation of an average Reynolds's equation is based on statistical properties of roughness height distribution [7-10]. Patir and Cheng [7] presented the average Reynolds equation for isotropic and directionally patterned surfaces. The flow factors for these surfaces were expressed as empirical relations in terms of hydrodynamic roughness parameter and surface pattern parameter. Majumdar and Hamrock [8] used this model for an EHL line contact problem. Sarangi et al. [9] applied Patir and Cheng model to examine the surface roughness effect on the stiffness and damping characteristics of EHL point contact. Chu et al. [10] studied the EHL point contact problem by considering the combined effect of surface roughness and flow rheology.

In the present work, the influence of surface roughness on the EHL finite line contact between axially profiled cylindrical roller and a flat plane has been studied using probabilistic model. In order to incorporate the surface roughness effect, the Reynolds equation is modified by using Patir and Cheng model [7]. The two contacting bodies are assumed to have identically structured surfaces. In this analysis, dub-off radius $\left(\bar{R}_y\right)$ is used as an edge profile (see Fig. 1).

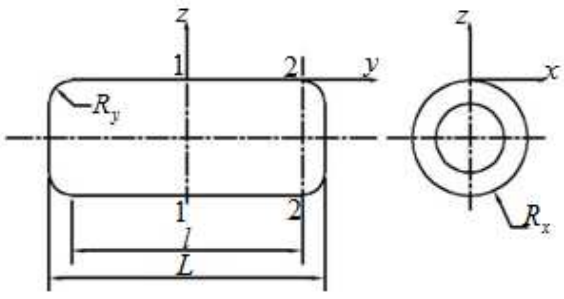

Fig. 1. Geometry of the cylindrical roller.

Modified Reynolds equation and the elastic deformation equation are solved numerically using multilevel method and multilevel multi-integration method, respectively. The differentials are discretized with finite difference method and solved iteratively for a preset convergence criterion. The results obtained from the finite and infinite line contact theories are compared. Based on numerically evaluated data, curve fitted relations for central film thickness (CFT) and central minimum film thickness (CMFT) are established by non-linear least square technique.

II. THEORY

Based on the Patir and Cheng model, the modified Reynolds equation for an isothermal steady-state finite line contact with incompressible Newtonian lubricant, including with Barus pressure-viscosity relationship [11] can be written as,

$$\frac{\partial}{\partial \bar{x}}\left(\xi_x \frac{\partial \bar{P}}{\partial \bar{x}}\right)+\frac{\partial}{\partial \bar{y}}\left(\xi_y \frac{\partial \bar{P}}{\partial \bar{y}}\right)=\frac{1}{2}\left[1+erf\left(\frac{\Lambda}{\sqrt{2}}\frac{\bar{h}}{\bar{h}_c}\right)\right]\frac{\partial \bar{h}}{\partial \bar{x}} \tag{1}$$

where, $\xi_x=\dfrac{\phi_x \bar{h}^3}{12\bar{U}\exp(G\bar{P})}$ and $\xi_y=\dfrac{\phi_y \bar{h}^3}{12\bar{U}\exp(G\bar{P})}$

The expressions for the flow factors are

$$\phi_x=\begin{cases}1-c_1 e^{-g(h/\sigma)} & \text{for } \gamma\le 1\\ 1+c_1\left(\dfrac{h}{\sigma}\right)^{-g} & \text{for } \gamma>1\end{cases} \tag{2}$$

and $\phi_y\left(\dfrac{h}{\sigma},\gamma\right)=\phi_x\left(\dfrac{h}{\sigma},\dfrac{1}{\gamma}\right)$

where, c_1 and g are constants and is given in reference [7]. γ is defined as the ratio of the lengths at which autocorrelation functions of the x and y profiles reduce to 50 percent of the initial values. The surface pattern parameter $\gamma<1$ corresponds to the surface having correlation length in the transverse direction, $\gamma=1$ corresponds to isotropic roughness pattern, while for longitudinal oriented surface $\gamma>1$. $\Lambda=\dfrac{h_c}{\sigma}$ measures the severity of roughness. From the expression of ϕ_x (equation (2)) it is noticed that when Λ approaches a large value, ϕ_x approaches 1. Then (1) reduced to classical Reynolds equation as applicable for a smooth surface. Variation of Λ is from 1 for a rough surface to 6 for a smooth surface. In the present work full film condition is assumed in which asperity contact does not take place. The load-supporting ability due to asperity contact will be prevailed for the value of Λ less than 0.5 **[9]**, which is not considered in the present analysis.

The film thickness equation is given by [5,6],

$$\begin{aligned}\bar{h}\left(\bar{x}_i,\bar{y}_j\right)&=\bar{h}_c-\bar{D}_c+\frac{\bar{x}_i^2}{2}+\bar{D}_{i,j} \quad \text{for } -\bar{l}/2\le \bar{y}_i\le \bar{l}/2\\ &=\bar{h}_c-\bar{D}_c+\frac{\bar{x}_i^2}{2}+\frac{\left(\bar{y}_j-\bar{l}/2\right)^2}{2\bar{R}_y}+\bar{D}_{i,j}\\ &\qquad \text{for } \bar{y}_j<-\bar{l}/2 \text{ and } \bar{y}_j>\bar{l}/2\end{aligned} \tag{3}$$

It is assumed that smaller wavelength roughness component remains unchanged; whereas, large wavelength roughness components deform almost completely [10]. The overall elastic deformation of element $\bar{D}_{i,j}$ due to the pressure at the corresponding $n_x \times n_y$ elements is given by,

$$\bar{D}_{i,j}=\frac{2}{\pi}\sum_{k=1}^{n_x}\sum_{l=1}^{n_y}\bar{P}_{k,l}K_{m,n} \tag{4}$$

where, $m=|k-i+1|$ and $n=|l-j+1|$

The expression of the influence coefficient $K_{m,n}$ is given as,

$$K_{m,n}=\left[\begin{aligned}&\left(x_m+\tilde{b}\right)\ln\left(\frac{y_n+\tilde{a}+\sqrt{\left(x_m+\tilde{b}\right)^2+\left(y_n+\tilde{a}\right)^2}}{y_n-\tilde{a}+\sqrt{\left(x_m+\tilde{b}\right)^2+\left(y_n-\tilde{a}\right)^2}}\right)\\ &+\left(x_m-\tilde{b}\right)\ln\left(\frac{y_n-\tilde{a}+\sqrt{\left(x_m-\tilde{b}\right)^2+\left(y_n-\tilde{a}\right)^2}}{y_n+\tilde{a}+\sqrt{\left(x_m-\tilde{b}\right)^2+\left(y_n+\tilde{a}\right)^2}}\right)\\ &+\left(y_n+\tilde{a}\right)\ln\left(\frac{x_m+\tilde{b}+\sqrt{\left(x_m+\tilde{b}\right)^2+\left(y_n+\tilde{a}\right)^2}}{x_m-\tilde{b}+\sqrt{\left(x_m-\tilde{b}\right)^2+\left(y_n+\tilde{a}\right)^2}}\right)\\ &+\left(y_n-\tilde{a}\right)\ln\left(\frac{x_m-\tilde{b}+\sqrt{\left(x_m-\tilde{b}\right)^2+\left(y_n-\tilde{a}\right)^2}}{x_m+\tilde{b}+\sqrt{\left(x_m+\tilde{b}\right)^2+\left(y_n-\tilde{a}\right)^2}}\right)\end{aligned}\right] \tag{5}$$

The non-dimensional load carrying capacity of the oil film can be determined by integrating the pressure over the contact envelope and it must be equal to the external applied load. This condition is generally referred to as force balance equation and is given by,

$$\bar{W}=\frac{1}{\bar{L}}\iint \bar{P}\,d\bar{x}\,d\bar{y} \tag{6}$$

III. NUMERICAL SOLUTION

The modified Reynolds's equation (1) and film thickness equation (3), which includes elastic deformation equation (4) is solved simultaneously by satisfying force balance equation (6) and fulfilling the boundary conditions. The pressure equation is solved by a multilevel method [12] and the elastic deformation is calculated with the multilevel multi-integration method [13]. The boundary conditions used are,

$$\bar{P}\left(\bar{x},-0.52\bar{L}\right)=\bar{P}\left(\bar{x},0.52\bar{L}\right)=0$$
$$\bar{P}\left(-6.5\bar{a},\bar{y}\right)=\bar{P}\left(2.5\bar{a},\bar{y}\right)=0 \quad (7)$$

In the present analysis Reynolds's cavitation condition is used which implies, $\bar{P}=\frac{\partial\bar{P}}{\partial\bar{x}}=\frac{\partial\bar{P}}{\partial\bar{y}}=0$ when $\bar{P}<0$.

Owing to the symmetry of the roller along the length, half of the domain is considered for the calculation. From the grid convergence analysis, the numbers of nodes adopted in the present work are 257 in rolling (x) direction and 1025 in transverse (y) direction. The Hertz pressure distribution is used as initial guess values of the solution of modified Reynolds equation. Gauss-Seidel line relaxation is used in the low pressure region and Jacobi distributive line relaxation is used in the high pressure region. The preset values of pressure ($\bar{P}$) convergence and load ($\bar{W}$) convergence are 10^{-5} and 10^{-3}, respectively.

Numerical solution of EHL infinite line contact including surface roughness effect is obtained according to the procedure given in [8]. The mesh size of 513 nodes is adopted for the infinite line contact analysis.

IV. RESULTS AND DISCUSSION

The geometrical configuration of the cylindrical roller used in the present work are $\bar{L}=2$ and $\bar{l}=1.4$. The range of the non-dimensional parameters studied are, speed parameter $\bar{U}=10\times10^{-12}$ to 210×10^{-12}, load parameter $\bar{W}=10\times10^{-6}$ to 50×10^{-6} and material parameter G = 2500 to 5000. The hydrodynamic roughness parameter (Λ) is varied from 1 to 10 and the values of surface pattern parameter (γ) examined are 1/6, 1/3, 1, 3, 6. In the present analysis, for the finite line contact case, the magnitude of central film thickness (CFT) and central minimum film thickness (CMFT) are extracted at the axial mid-span of roller (see section line 1-1 in Fig. 1); whereas, the minimum film thickness (MEFT) is obtained at the edges of the roller (section line 2-2 in Fig. 1). CMFT is the conventional minimum film thickness as obtained in the case of infinite line contact analysis and MEFT is a minimum value of the film thickness in the whole contact region, generally found at the edges.

In order to check the accuracy of numerical computation, the results of smooth surface contact ($\gamma=1$, $\Lambda=6$) are compared (see Fig. 2). The numerical data used are, $\bar{W}=10\times10^{-6}$, $G=2500$, $\bar{R}_y$=0.3, γ=1, Λ=6. Good agreement is obtained between the present numerical prediction and extrapolated CFT and CMFT formulae of Dowson and Toyoda [14]. Comparison is also made with the available data of CMFT and MEFT values presented by Park and Kim [5]. A small difference in the values is observed, may be due to the consideration of compressible flow in [5].

The effect of hydrodynamic roughness parameter (Λ) on the pressure distribution and film thickness profile at a constant load is studied for an isotropic roughness ($\gamma=1$). With a decrease in Λ, the resistance to the flow increases which improves the pressure development and thereby enhancing the load carrying capacity. Since, in the present case the load is kept constant; it is expected that for decreasing value of Λ (smooth $\Lambda=6$ to rough $\Lambda=2$) the film thickness should increase in order to balance the load, which is also observed in Fig. 3.

The influence of surface pattern parameter (γ) on the pressure distribution and film thickness profile at a constant load is studied for a rough surface $(\Lambda=3)$. The transverse roughness $(\gamma<1)$ offers maximum resistance to the flow; whereas longitudinal roughness $(\gamma>1)$ provides minimum flow resistance.

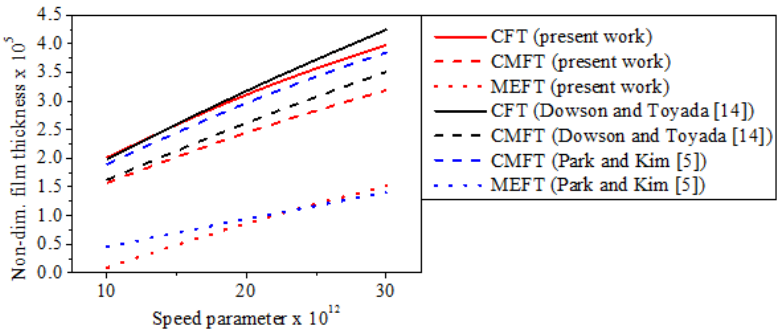

Fig. 2. Comparison of film thickness.

This implies transverse roughness generates higher pressure in compare to isotropic and longitudinal roughness. Therefore, load capacity for transverse roughness is greater than isotropic and longitudinal roughness. Under constant load condition, it is evident that the film thickness for transverse roughness is higher while the longitudinal roughness $(\gamma > 1)$ produces the lower film thickness, as shown in Fig. 4.

The results obtained from EHL finite and infinite theories are compared. Infinite line contact theory takes into account a flow factor in the rolling direction alone (ϕ_x in 1-D Reynolds equation) to include roughness effect. Since finite line contact theory considers both the flow factors (ϕ_x and ϕ_y in 2-D Reynolds equation) which increases the overall resistance to the flow for the transverse and isotropic surface roughness pattern; whereas, for longitudinal surface roughness pattern overall resistance to the flow gets decreased. Probably, for this reason there is a difference in the results obtained from finite and infinite line contact theories. Under fixed load condition, Figs. 3-4 indicate that for a transverse and isotropic roughness the film thickness results of finite line contact are substantially higher as compared to infinite line contact. However, for longitudinal roughness the film thickness obtained using finite line contact theory is significantly lower than the infinite line contact solution. Furthermore, it is also noticed that the pressure profile of a finite line contact is wider in the contact zone; the pressure spike is lower and shifted towards the exit zone as compared to infinite line contact results.

Fig. 5 shows the effect of hydrodynamic roughness parameter (Λ) on the film thickness (CFT and CMFT) at a constant load for different surface pattern parameter ($\gamma = 1/6,\ 1,\ 6$). It is observed that with a decrease in Λ, there is an increase in the film thickness for transverse and isotropic roughness, whereas for longitudinal roughness the film thickness decreases. For all three types of surface roughness, the film thickness converges to the smooth surface value at $\Lambda = 6$. A significant difference is noticed in the film thickness results of finite and infinite contact, particularly for lower values of Λ.

The effect of edge radius $\bar{R}_y$ on the film thickness and maximum pressure is shown in Fig. 6. The variation of an edge radius has a negligible effect on the CFT, CMFT and central pressure. However, there is significant rise in the MEFT and considerable reduction in edge pressure, with increase in edge radius. Therefore, one should use maximum possible value of edge radius, to minimize the pressure along the edges of roller. It is also observed that for a rough surface, the film thickness values are considerably higher and the maximum pressure is slightly lower as compared to smooth surface results. It should be noted that the maximum edge pressure is significantly higher than the maximum central pressure.

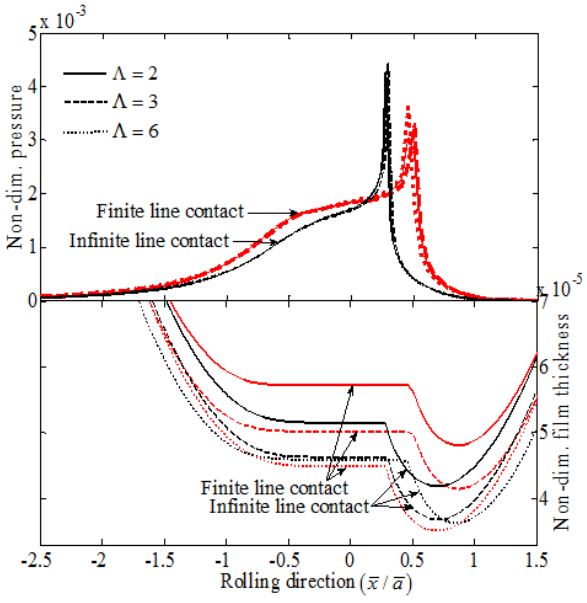

Fig. 3. Pressure and film thickness profile at section line 1-1 (Fig. 1) for isotropic roughness pattern ($\gamma = 1$) at

$\bar{W} = 15\times10^{-6},\ \bar{U} = 20\times10^{-12},\ G = 5000,\ \bar{R}_y = 0.8$

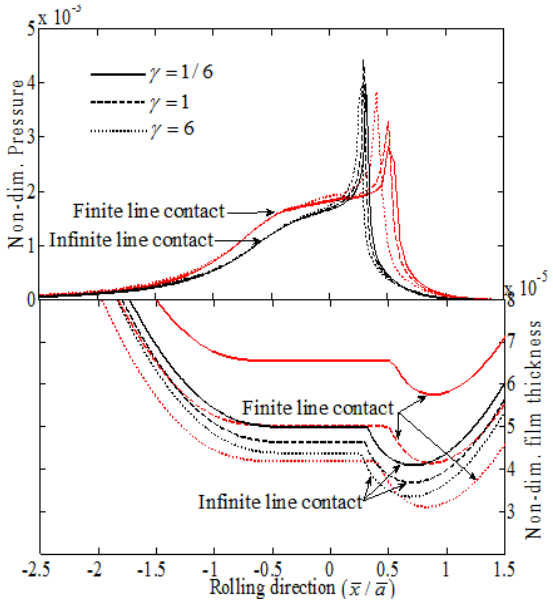

Fig. 4. Pressure and film thickness profile at section line 1-1 (Fig. 1) for the case of rough surface ($\Lambda = 3$) at

$\bar{W} = 15\times10^{-6},\ \bar{U} = 20\times10^{-12},\ G = 5000,\ \bar{R}_y = 0.8$

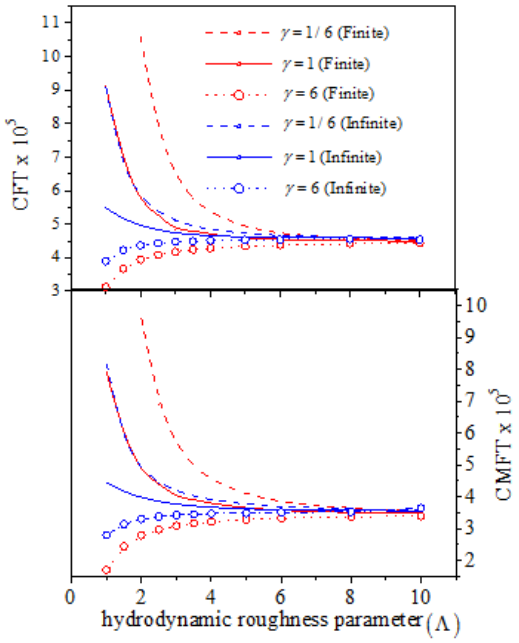

Fig. 5. Effect of hydrodynamic roughness parameter (Λ) on the film thickness at

$\bar{W} = 15\times10^{-6}$, $\bar{U} = 20\times10^{-12}$, $G = 5000$, $\bar{R}_y = 0.8$

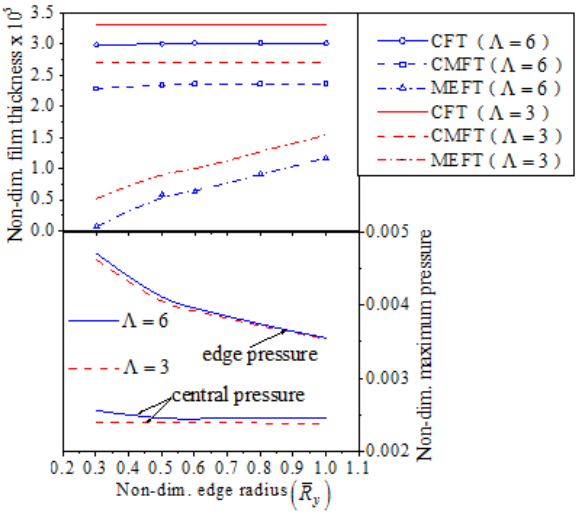

Fig. 6. Non-dimensional pressure and film thickness variation with edge radius $(\bar{R}_y)$ at

$\bar{W} = 22.5\times10^{-6}$, $\bar{U} = 20\times10^{-12}$, $G = 2500$, γ=1

V. EMPIRICAL FORMULAE

The existing relations to evaluate CFT and CMFT are based on EHL infinite line contact theory and are applicable for smooth surfaces. Therefore, new relations are developed from the numerical results obtained by varying the non-dimensional parameters ($\bar{W}, \bar{U}, G, \Lambda, \gamma$). Nonlinear least-square regression technique is used for the correlation of numerical and curve fitted values. The derived curve fitted relations are,

$$\bar{h}_c = a_1 G^{a_2} \bar{U}^{a_3} \bar{W}^{a_4} \left(\Lambda^{a_5} - a_6 \left(\exp\left(\Lambda^{a_7} \right) \right)^{a_8 \gamma} \right) \quad (8)$$

$$\bar{h}_{cm} = b_1 G^{b_2} \bar{U}^{b_3} \bar{W}^{b_4} \left(\Lambda^{b_5} - b_6 \left(\exp\left(\Lambda^{b_7} \right) \right)^{b_8 \gamma} \right) \quad (9)$$

$\bar{h}_c$ and $\bar{h}_{cm}$ are the non-dimensional CFT and CMFT, respectively. The constants and exponents of various dimensionless parameters in the above equations are given in the Table I and II. From the Figs. 7-9, it is observed that curve fitted data obtained from the curve fitted relations are in close agreement with the numerically calculated values.

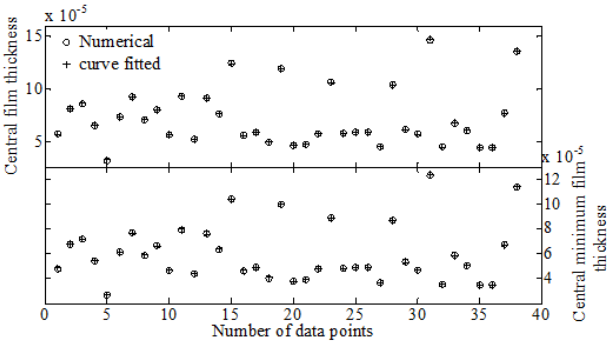

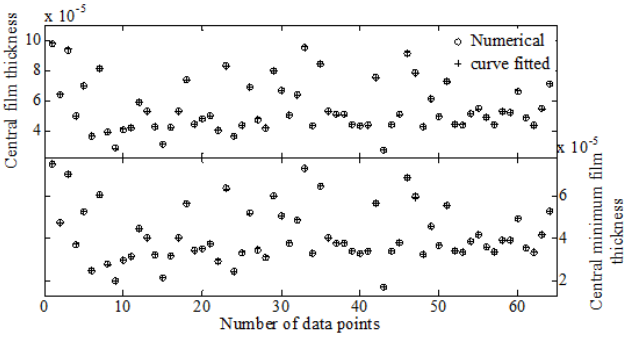

The power constants of $\bar{W}$, $\bar{U}$, G corresponding to curve fitted relations are close to the Dowson and Toyoda formulae [14], comprising with the additional terms to incorporate the surface roughness effect. For the design purpose, a quick evaluation of central and central minimum film thickness is possible with the use of curve

Fig. 7. Curve fitting of non-dimensional CFT and CMFT for an isotropic roughness pattern.

Fig. 8. Curve fitting of non-dimensional CFT and CMFT for a longitudinal roughness pattern.

fitted relations obtained from the present work; which are applicable for moderated loads (within the range of non-dimensional parameters as mentioned in sec. IV).

Few calculated values of the film thickness from the derived curve fitted relations are compared with Dowson and Toyoda formulae [14] ($\bar{h}_c = 3.06G^{0.56}\bar{U}^{0.69}\bar{W}^{-0.1}$, $\bar{h}_{cm} = 2.67G^{0.54}\bar{U}^{0.7}\bar{W}^{-0.13}$) for the case of smooth surface and are given in the Table III. There is a close agreement between the film thickness values obtained from the present formulae and Dowson and Toyoda formulae. Therefore, present formulae are applicable for smooth as well as rough surfaces.

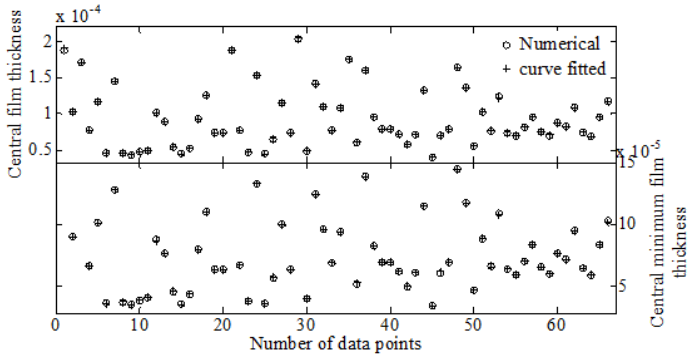

Fig. 9. Curve fitting of non-dimensional CFT and CMFT for a transverse roughness pattern.

TABLE I. CONSTANTS AND EXPONENTS OF VARIOUS DIMENSIONLESS PARAMETERS USED IN CURVE FITTED RELATIONS OF THE CFT ($\bar{h}_c$)

Roughness	a_1	a_2	a_3	a_4	a_5	a_6	a_7	a_8
Isotropic $\gamma = 1$	1.558	0.537	0.6301	-0.065	-1.582	-0.244	0.063	1
Transverse $\gamma = 1/6, 1/3$	16.336	0.557	0.6634	-0.084	-2.399	-0.113	-2.729	-14.834
Longitudinal $\gamma = 3, 6$	1.201	0.566	0.6736	-0.077	-0.021	-1.129	-1.620	-0.156

TABLE II. CONSTANTS AND EXPONENTS OF VARIOUS DIMENSIONLESS PARAMETER USED IN CURVE FITTED RELATIONS OF CMFT ($\bar{h}_{cm}$)

Roughness	b_1	b_2	b_3	b_4	b_5	b_6	b_7	b_8
Isotropic $\gamma = 1$	1.927	0.548	0.645	-0.072	-1.216	-0.140	0.133	1
Transverse $\gamma = 1/6, 1/3$	15.619	0.566	0.672	-0.089	-2.217	-0.099	-2.782	-23.128
Longitudinal $\gamma = 3, 6$	0.173	0.580	0.686	-0.093	-0.624	-10.945	-1.708	-0.146

TABLE III. COMPARISON OF FILM THICKNESS FOR THE CASE OF SMOOTH SURFACE ($\gamma = 1$, $\Lambda = 6$) DETERMINED FROM THE DERIVED CURVE FITTED RELATIONS, WITH THAT OF DOWSON AND TOYODA FORMULAE

Sr. No	G	$\bar{W}$ x 10^6	$\bar{U}$ x 10^{12}	**CFT**		**CMFT**	
				Present formula x 10^5	***Dowson and Toyoda*** x 10^5	***Present formula*** x 10^5	***Dowson and Toyoda*** x 10^5
1	5000	30	20	4.3381	4.2378	3.3685	3.3316
2	2500	25	30	3.9076	3.8725	3.0309	3.1164
3	4000	45	60	7.4894	7.6644	5.8782	6.0452
4	2500	35	20	2.9608	2.8306	2.2781	2.2459
5	2500	10	10	2.0761	1.9887	1.5942	1.6270

VI. CONCLUSION

A numerical solution to the isothermal EHL finite line contact including the surface roughness effect is reported. In the present analysis, Patir-Cheng flow model of two identically structured surfaces is incorporated. Results indicate that the maximum pressure and minimum film thickness occurs near the edges of the roller, which can be controlled by proper selection of the edge radius. In comparison to infinite line contact results, the pressure profile of a finite line contact is wider in the contact zone; the pressure spike is lower and shifted towards the exit zone. A significant difference in the film thickness results of finite and infinite contact are reported, particularly for lower values of hydrodynamic roughness parameter Λ. Finally, curve fitted relations for an estimation of non-dimensional central film thickness (CFT) and central minimum film thickness (CMFT) are derived under various operating conditions.

REFERENCES

[1] M. Feng and G. Yan, "Stress analysis of the skewed-roller slipping clutch based on frictional contact and dynamic equilibrium," Applied Mechanics and Materials, vol. 86, pp. 850–853, 2011.

[2] P.M. Johns and R. Gohar, "Roller bearings under radial and eccentric loads," Tribol. Int., pp. 131-136, 1981.

[3] D.G. Wymer and A. Cameron, "Elastohydrodynamic lubrication of a line contact," Proc. IMechE., vol. 188, pp. 221–238, 1973.

[4] A, Mostofi and R. Gohar, " Elastohydrodynamic lubrication of finite line contacts," Transactions of the ASME J Lubric. Technol., vol. 105, pp. 598–604, 1983.

[5] T.J Park and K.W. Kim, "Elastohydrodynamic lubrication of a finite line contact," Wear, vol. 223, pp. 102–109, 1998.

[6] X. Liu and P. Yang, "Analysis of the thermal elastohydrodynamic lubrication of a finite line contact," Tribol. Int., vol. 35, pp. 137–144, 2002.

[7] N. Patir and H.S. Cheng, "An average flow model for determining effects of three-dimensional roughness on partial hydrodynamic lubrication," Transactions of the ASME J Lubric. Technol., vol. 100, pp. 12–17, 1978.

[8] B.C. Majumdar and B.J. Hamrock, "Effect of surface roughness on elastohydrodynamic line contact," Transactions of the ASME J Lubric. Technol., vol. 104, pp. 401–408, 1982.

[9] M. Sarangi, B.C. Majumdar, and A.S. Sekhar, "Stiffness and damping characteristics of lubricated ball bearings considering the surface roughness effect Part 2: numerical results and application," Proc. Instn Mech. Engrs, Part J, Journal of Engineering Tribology, vol. 218, pp. 539–547, 2004.

[10] L.M. Chu, W.L. Li, J.R. Lin, and Y.P. Chang, "Coupled effect of surface roughness and flow Rheology on elastohydrodynamic lubrication," Tribol. Int., vol. 43, pp. 483–490, 2010.

[11] C. Barus, "Isotherms, isopiestics and isometrics relative to viscosity," Am. J. Sci., vol. 45, pp. 87–96, 1893.

[12] C.H. Venner, "Multilevel solution of the EHL line and point contact problems," Ph.D. Thesis, University of Twente, Netherlands, 1991.

[13] A. Brandt and A.A. Lubrecht, "Multilevel matrix multiplication and fast solution of integral equations," J Comput. Phys., vol. 90, pp. 348–70, 1990.

[14] D. Dowson and SA. Toyoda, "Central Film Thickness Formula for Elastohydrodynamic Line Contacts," Proceedings of 5th Leeds-Lyon Symp. Mechanical Engineering Publication, Leeds, England, pp. 60–67, 1977.

NOMENCLATURE

a , $\bar{a}$ = Half width of Hertzian contact, $\bar{a} = a / R_x$

D, D_c =combined elastic deformation and central elastic deformation, $\bar{D} = D / R_x$

E' =combined Young's modulus,

G =material parameter, $G = \alpha E'$

$h, \bar{h}$ =film thickness, $\bar{h} = h / R_x$

$h_c, \bar{h}_c$ =central film thickness, $\bar{h}_c = h_c / R_x$

h_{cm} = central minimum film thickness

h_m = minimum film thickness

$L, \bar{L}$ =length of cylindrical roller, $\bar{L} = L / R_x$

$l, \bar{l}$ =length of the straight part of roller, $\bar{l} = l / R_x$

$p, \bar{P}$ =hydrodynamic pressure, $\bar{P} = p / E'$

R_x =radius of cylindrical roller.

$R_y, \bar{R}_y$ =radius of the end profile of the roller, $\bar{R}_y = R_y / R_x$

u_a, u_b =surface velocity in the direction of rolling,

$$U = \frac{(u_a + u_b)}{2} \, , \bar{U} = \eta_0 U / (E' R_x)$$

$W, \bar{W}$ =load capacity, $\bar{W} = W / (E' L R_x)$

$x, y, \bar{x}, \bar{y}$ =referred coordinate axes,

$$\bar{x} = x / R_x \text{ and } \bar{y} = y / R_x$$

α =pressure-viscosity coefficient of lubricant.

γ = surface pattern parameter

η, η_0 =absolute viscosity of the lubricant

Λ = hydrodynamic roughness parameter

ν_1, ν_2 = Poisson's ratio of roller and flat surface respectively

σ = combined standard deviation of roughness

ϕ_x, ϕ_y = flow factors

$2\tilde{a}$ = Step size in *y*-direction

$2\tilde{b}$ = Step size in *x*-direction